HHS Public Access

Author manuscript

Sci Transl Med. Author manuscript; available in PMC 2016 February 26.

Published in final edited form as:

Sci Transl Med. 2015 March 4; 7(277): 277ra31. doi:10.1126/scitranslmed.aaa0154.

Paroxetine-mediated GRK2 inhibition reverses cardiac dysfunction and remodeling after myocardial infarction

Sarah M. Schumacher[1,2], **Erhe Gao**[1], **Weizhong Zhu**[3], **Xiongwen Chen**[3], **J. Kurt Chuprun**[1,2], **Arthur M. Feldman**[3], **John J. G. Tesmer**[4], and **Walter J. Koch**[1,2,*]

[1]Center for Translational Medicine, Temple University School of Medicine, Philadelphia, PA 19140, USA

[2]Department of Pharmacology, Temple University School of Medicine, Philadelphia, PA 19140, USA

[3]Cardiovascular Research Center, Temple University School of Medicine, Philadelphia, PA 19140, USA

[4]Life Sciences Institute, University of Michigan, Ann Arbor, MI 48109, USA

Abstract

Heart failure (HF) is a disease of epidemic proportion and is associated with exceedingly high health care costs. G protein (heterotrimeric guanine nucleotide–binding protein)–coupled receptor (GPCR) kinase 2 (GRK2), which is up-regulated in the failing human heart, appears to play a critical role in HF progression in part because enhanced GRK2 activity promotes dysfunctional adrenergic signaling and myocyte death. Recently, we found that the selective serotonin reuptake inhibitor (SSRI) paroxetine could inhibit GRK2 with selectivity over other GRKs. Wild-type mice were treated for 4 weeks with paroxetine starting at 2 weeks after myocardial infarction (MI). These mice were compared with mice treated with fluoxetine, which does not inhibit GRK2, to control for the SSRI effects of paroxetine. All mice exhibited similar left ventricular (LV) dysfunction before treatment; however, although the control and fluoxetine groups had continued degradation of function, the paroxetine group had considerably improved LV function and structure, and several hallmarks of HF were either inhibited or reversed. Use of genetically

*Corresponding author: walter.koch@temple.edu.

Author contributions: S.M.S. and W.J.K. wrote the manuscript and designed the experiments. S.M.S. conducted most of the experiments and analyzed the data. E.G. performed the sham and MI surgeries as well as in vivo hemodynamics. S.M.S. and E.G. performed statistical analysis. W.Z. prepared membrane fractions and performed the radioligand binding assay and measurements. X.C. isolated adult mouse cardio-myocytes and performed and analyzed the single myocyte contraction assay. W.Z., X.C., J.K.C., A.M.F., J.J.G.T., and W.J.K. provided intellectual guidance and manuscript revision.

Competing interests: The authors declare that they have no competing interests.

SUPPLEMENTARY MATERIALS

www.sciencetranslationalmedicine.org/cgi/content/full/7/277/277ra31/DC1

Detailed Methods

Fig. S1. Paroxetine restores βAR mRNA expression.

Fig. S2. Paroxetine enhances myocyte contraction in response to ISO in control, but not in βARKct transgenic myocytes.

Fig. S3. Paroxetine reduces LV dimension despite elevated GRK2 levels.

Fig. S4. Paroxetine's beneficial effect in post-MI HF is maintained after termination of treatment.

Table S1. Reduction of LV dimension by paroxetine is not additive with GRK2 inhibition by βARKct.

Source Data (Excel file)

engineered mice indicated that paroxetine was working through GRK2 inhibition. The beneficial effects of paroxetine were markedly greater than those of β-blocker therapy, a current standard of care in human HF. These data demonstrate that paroxetine-mediated inhibition of GRK2 improves cardiac function after MI and represents a potential repurposing of this drug, as well as a starting point for innovative small-molecule GRK2 inhibitor development.

INTRODUCTION

With about 550,000 new cases of heart failure (HF) diagnosed in the United States alone each year, this disease represents a growing health care concern (1). Despite substantial improvements in its management, including improved mechanical and pharmacological therapy, outcomes in HF remain poor (1). Thus, there is an urgent need to develop new therapeutic strategies, including cell- and gene-based therapies, and recent research has been aimed at the underlying mechanisms of HF progression.

A main driving force in the pathophysiology of HF is an increased sympathetic drive, which occurs to stimulate failing pump function. Although elevated norepinephrine causes an initial compensatory increase in heart rate (HR) and cardiac output, prolonged sympathetic nervous system (SNS) activation participates in the progressive, maladaptive changes characteristic of HF (2, 3). One mechanism by which increased circulating catecholamine levels contribute to HF progression is through dysregulation of GPCR [G protein (heterotrimeric guanine nucleotide–binding protein)–coupled receptor] function in the heart. Enhanced stimulation of β-adrenergic receptors (βARs) followed by increased activation of GPCR kinases (GRKs) leads to enhanced phosphorylation, internalization, and down-regulation of βAR density and signaling, leading to a loss in inotropic reserve (4, 5). In particular, in failing human hearts, the levels and activity of GRK2 are elevated (6, 7). Increased GRK2 has been shown to participate in adverse remodeling and contractile dysfunction during HF, whereas GRK2 inhibition through a C-terminal peptide that competes with GRK2 binding to Gβγ (βARKct) enhances heart function and can prevent and reverse HF (8–14). Further, GRK2 is a pro-death kinase in the heart, inhibiting vital cell survival pathways and promoting apoptosis after cardiac injury (15–17). These data present compelling evidence of a causal role for GRK2 in the maladaptive progression of cardiac remodeling and dysfunction leading to HF, especially after ischemic injury. Therefore, the development of small-molecule inhibitors of GRK2 appears warranted for pharmacologic treatment of HF.

Recently, we discovered that the selective serotonin reuptake inhibitor (SSRI) antidepressant drug paroxetine specifically bound to the catalytic domain of GRK2 as an off-target and inhibited kinase activity in the micromolar range of affinity (18). Further, paroxetine could inhibit GRK2 with selectivity over other GRK subfamilies (18). Moderate concentrations of paroxetine inhibited GRK2 target phosphorylation in vitro and significantly potentiated the βAR-mediated increase in myocardial contractility in vitro and in vivo after isoproterenol (ISO) administration (18). Here, we directly investigated whether paroxetine-mediated inhibition of GRK2 could improve cardiovascular signaling and function in a mouse model of HF.

RESULTS

Chronic paroxetine treatment improves cardiac function after myocardial infarction

To determine whether pharmacologic inhibition of GRK2 by paroxetine could provide improvement in cardiac function in an animal model of HF, wild-type C57BL/6 mice underwent myocardial infarction (MI) or sham surgery (19) and were allowed 2 weeks for infarct development and HF progression before 4 weeks of treatment with vehicle [dimethyl sulfoxide (DMSO) in water], paroxetine, or fluoxetine (both at 5 mg/kg per day) through subcutaneous miniosmotic pumps. These doses were determined on the basis of a literature search of murine studies investigating their SSRI effects, in which doses ranged from 1 to 10 mg/kg. Using this treatment protocol, we found that the serum paroxetine levels ranged between 27 and 192 ng/ml after 4 weeks of treatment in both sham and post-MI animals (n = 6 per group, control serum from vehicle-treated animals was below the low limit of detection of 1 ng/ml). Quantitative determinations of paroxetine concentration in human serum have revealed that over clinically relevant doses used for depression (10 to 60 mg/day), levels range between 5 and 190 ng/ml (20–22), indicating that levels in our HF mice are equivalent.

All post-MI mice exhibited similar cardiac function at baseline and 2 weeks after MI (Fig. 1). For example, left ventricular (LV) ejection fraction (EF) decreased from ~70 to ~35% after 2 weeks, which is characteristic of post-MI hearts (Fig. 1, A and B). In contrast to the continuing degradation of function and structure in the vehicle- and fluoxetine-treated groups, paroxetine treatment led to robust improvement (Fig. 1). Paroxetine produced an ~30% absolute increase in EF and an ~20% absolute increase in fractional shortening (FS) above vehicle at 6 weeks after MI (Fig. 1, B and C). Analysis of LV internal diameter during diastole (LVIDd) and systole (LVIDs) revealed a significant restoration of LV dimension with paroxetine treatment (Fig. 1, D and E). In addition, LV end-diastolic dimension (LVEDd) was significantly preserved with paroxetine (Fig. 1F).

At 6 weeks after MI, cardiovascular function and adrenergic responsiveness were analyzed through terminal hemodynamics at baseline and upon challenge with increasing doses of the βAR agonist ISO (Fig. 2). No difference was observed in mean systemic pressure (Fig. 2B) or HR responses to ISO (Fig. 2C), consistent with previous studies that observed no changes in pressure or HR with GRK2 lowering (8, 23). Although there was no statistical difference at baseline, paroxetine enhanced dP/dt maximum and minimum at every dose of ISO in treated sham animals (Fig. 2, D and E). Paroxetine enhanced contractility after MI (Fig. 2, D and E). Furthermore, the nearly 2.5-fold increase in LV end-diastolic pressure (LVEDP) after MI, as a physiological index of HF, in the vehicle and fluoxetine groups was completely and selectively blocked with paroxetine (Fig. 2F).

Paroxetine treatment limits adverse ventricular remodeling after MI

We next investigated whether the enhanced cardiac function seen with chronic paroxetine treatment was due in part to reduced or reversed maladaptive remodeling of the LV, consistent with GRK2 lowering (13, 14). Heart weight (HW) and length (HL) normalized to tibia length (TL) were significantly reduced in paroxetine-treated post-MI mice compared to

vehicle-and fluoxetine-treated controls (Fig. 3, A and B). Further, the about twofold increase in lung weight (LW) in the vehicle and fluoxetine groups, showing evidence of HF development, was totally normalized by paroxetine treatment (Fig. 3C). To visualize scar formation and fibrosis, we harvested hearts 6 weeks after MI, and paraffin-embedded sections were stained with Masson's trichrome. Although no difference was observed in sham hearts, preservation of LV architecture was evident in trichrome-stained, four-chamber sections of post-MI hearts treated with paroxetine (Fig. 3D). Four-chamber images were taken at the level of the aortic outflow tract where the long and short axes of the LV are maximum, for quantitative comparison. Only paroxetine treatment significantly reduced luminal area after MI (Fig. 3F).

To investigate the integrity of the myocardium, we collected higher-magnification images of the border zone (×10), transitional zone (×20), and infarct area (×10) (Fig. 3G). These images revealed a substantial reduction in fibrosis in the border zone of paroxetine-treated post-MI hearts, as well as a potential preservation of cardiomyocyte microstructure in the border zone and myocyte content in the infarct zone. Together, these data suggest that paroxetine inhibition of GRK2 preserves the structural integrity of the myocardium.

Paroxetine treatment reverses SNS overdrive and normalizes the myocardial β-adrenergic system after MI

Sympathetic overdrive in injured and compromised myocardium can increase GRK2 levels, which enhances βAR down-regulation in chronic HF through increased phosphorylation and internalization (2, 4). To determine whether paroxetine therapy can prevent or reverse sympathetic overdrive in the post-MI mouse, we measured serum catecholamine levels from sham and 6-week post-MI animals (Fig. 4, A and B). Although serum epinephrine and norepinephrine levels were significantly enhanced 6 weeks after MI in animals treated with vehicle or fluoxetine, they were restored to near sham levels with paroxetine treatment (Fig. 4, A and B). To assess whether paroxetine therapy and its catecholamine-lowering properties translate to restoration of βAR density, we used radioligand binding and found that at 6 weeks after MI, there is significant βAR down-regulation as expected (Fig. 4C). Four weeks of paroxetine treatment was found to restore βAR density to near sham levels (Fig. 4C). We also found similar restoration of βAR mRNA in these samples (fig. S1). These data agree with the restoration of βAR sensitivity observed during hemodynamic analysis in these animals in Fig. 2 and are consistent with paroxetine inhibiting the nodal regulator of cardiac βAR dysfunction—GRK2 (13). Finally, to complete the mechanistic circuit of GRK2 inhibition in the failing heart, we found that paroxetine treatment, but not fluoxetine treatment, reduced myocardial GRK2 protein up-regulation seen 6 weeks after MI (Fig. 4D).

Cardiac-specific GRK2 gain- and loss-of-function mice support paroxetine's therapeutic mechanism after MI as GRK2 inhibition

Our laboratory has previously shown that myocardial expression of a C-terminal peptide of GRK2 (βARKct), which competes for Gβγ binding and subsequent membrane translocation and activation, can enhance heart function and prevent as well as reverse HF in both small and large animals (9, 12). To prove that paroxetine is indeed exerting beneficial effects after MI through inhibition of this pathological kinase, we used cardiac-targeted βARKct

transgenic mice (TgβARKct) as well as cardiac GRK2–overexpressing mice (TgGRK2), where levels of GRK2 are similar to those observed in human HF (8). First, TgβARKct and their non-transgenic littermate control (NLC) mice were treated with MI or sham surgery as above and then treated for 4 weeks with paroxetine (5 mg/kg per day) beginning 2 weeks after MI. Consistent with previous studies, cardiac function (LVEF) was significantly improved in TgβARKct mice 2 weeks after MI compared to NLC mice (Fig. 5A). As seen above, paroxetine enhanced function in post-MI NLC mice after 4 weeks of treatment (6 weeks after MI); however, it had no additional effects in post-MI TgβARKct mice over existing GRK2 inhibition (Fig. 5A). Consistent with these results and the in vivo GRK2 targeting of paroxetine, when isolated myocytes from NLC and TgβARKct mice were studied, the enhanced ISO-mediated contractile actions of paroxetine were absent when GRK2 was already inhibited by βARKct expression (fig. S2).

Similar to the above in vivo cardiac functional effects, LVIDd and LVIDs were considerably improved in vehicle-treated TgβARKct post-MI mice; however, the positive effects of paroxetine were only found in post-MI NLC mice with no additional therapeutic benefit in TgβARKct mice (table S1). In agreement, HW/TL and LW/TL were increased only in vehicle-treated NLC mice 6 weeks after MI, but preserved in TgβARKct animals independent of treatment and restored in NLC mice with paroxetine (Fig. 5, B and C). Thus, the GRK2 inhibitory actions of paroxetine in post-MI mice are equivalent to βARKct-mediated inhibition of this kinase.

To investigate whether the therapeutic effects of paroxetine are still present when GRK2 is up-regulated before MI, which would model the clinical scenario of treating existing HF patients, we studied TgGRK2 mice and their corresponding NLCs. Under the identical experimental protocol as above, post-MI TgGRK2 mice showed considerably more cardiac dysfunction after 2 weeks compared to NLC mice (Fig. 5D), consistent with the pathological nature of this kinase in injured myocardium. Despite an overall greater degree of dysfunction in vehicle-treated TgGRK2 hearts 6 weeks after MI compared to NLC, paroxetine treatment restored LVEF in TgGRK2 hearts to that of NLC (Fig. 5D). LV dilation was also greater in vehicle-treated TgGRK2 versus NLC mice at 2 and 6 weeks after MI as measured by LVIDs, but LV dimension was restored in both upon paroxetine treatment (fig. S3, A and B). In agreement, although HW/TL was greater in vehicle-treated TgGRK2 mice compared to NLC mice, cardiac hypertrophy was completely restored in paroxetine-treated mice 6 weeks after MI (Fig. 5E). Increased LW was also normalized in these post-MI mice after 4 weeks of paroxetine treatment (Fig. 5F). Overall, paroxetine treatment was no less effective at reducing LV dysfunction in TgGRK2 animals than in wild-type mice, validating its therapeutic potential despite a less favorable biochemical cardiac milieu when this pathological enzyme is enhanced.

Inhibition of GRK2 activity by paroxetine signaling demonstrates a persistent beneficial effect after MI

To investigate whether the improved cardiac function, reverse remodeling, and resetting of SNS overdrive and myocardial β-adrenergic signaling seen after 4 weeks of paroxetine treatment in post-MI mice were persistent, we studied a cohort of animals 2 weeks after

termination of vehicle or paroxetine treatment (8 weeks after MI). The paroxetine-mediated increase in EF and LV +/−d*P*/d*t* maximum and minimum post-MI was maintained 2 weeks after cessation of treatment (Fig. 6, A and B, and fig. S4). Furthermore, the 2.5-fold increase in LVEDP in the vehicle-treated post-MI group was completely reversed with paroxetine (fig. S4). The improvement in HW and LW was also preserved after 2 weeks of no treatment in the post-MI mice previously receiving paroxetine (Fig. 6, C and D), and no increase was observed in induction of the fetal gene program (fig. S4). Analysis of serum catecholamine levels revealed a maintenance near sham values in post–paroxetine treatment mice despite a more pronounced elevation in the vehicle group (Fig. 6, E and F). These data are consistent with paroxetine normalizing the SNS/β-adrenergic axis after 4 weeks of treatment in these mice (Fig. 4), which apparently can preserve the improvement in cardiac function and structure even after acute GRK2 inhibition is stopped.

Paroxetine treatment demonstrates therapeutic translational potential above and beyond current standard of care

To increase the translational relevance of a potential repurposing of paroxetine for HF therapy, at least in a depressed population, we carried out an experiment to evaluate its post-MI effectiveness compared to a current human HF standard of care, βAR blockade. To do this, mice at 2 weeks after MI were treated for 4 weeks with vehicle, the clinically used β_1-AR antagonist metoprolol at 250 mg/kg per day, paroxetine at 5 mg/kg per day, or both drugs concurrently. In contrast to the progressive contractile dysfunction in vehicle-treated mice, metoprolol treatment stabilized LV function, maintaining EF and FS with no further deterioration from 2 to 6 weeks after MI (Fig. 7, A and B). Metoprolol did not improve function, whereas paroxetine treatment alone or its co-administration with metoprolol demonstrated a reversal of LV dysfunction, significantly improving EF and FS after MI (Fig. 7, A and B). Finally, metoprolol treatment alone reduced but did not prevent the continued expansion of LVIDd and LVIDs (Fig. 7, C and D). In contrast, paroxetine alone or cotherapy with paroxetine and metoprolol significantly improved LV dimension (Fig. 7, C and D). When looking at the structure of the dissected heart, HW/TL ratios were reduced in all treatment groups (Fig. 7E), and LW as a measure of HF was also reduced by all three treatments with the trend for paroxetine to be most effective (Fig. 7F).

Finally, the molecular characteristics of HF were assessed in 6-week post-MI hearts to determine whether biomarkers of HF were reduced with 4 weeks of paroxetine treatment compared to β-blocker therapy. In Fig. 4, paroxetine can have a positive effect on SNS and β-adrenergic signaling, including a decrease in GRK2 levels in the heart, leading to improved cardiac function. Under our experimental conditions, metoprolol alone was less effective at lowering GRK2 compared to post-MI treatment when paroxetine was given (Fig. 8A). One characteristic of HF is the myocardial reactivation of fetal gene expression, and some of these, such as atrial natriuretic factor (ANF) and brain natriuretic peptide (BNP), have been used as HF biomarkers. Therefore, we assessed the gene expression of ANF and BNP, as well as β-myosin heavy chain (βMHC), which is also an HF marker, through reverse transcription polymerase chain reaction (RT-PCR) in 6-week post-MI hearts to determine whether these molecular markers of HF were reduced with paroxetine or β-blocker therapy. Metoprolol therapy alone was not able to reduce significantly the induction

of the fetal gene program, whereas paroxetine alone was able to reduce the mRNA expression of all three fetal genes (Fig. 8. B to D). Overall, these data demonstrate that paroxetine inhibition of GRK2 preserves the cardiac functional, structural, and biochemical integrity of the myocardium after MI to a greater extent than β-blocker therapy.

DISCUSSION

Herein, we investigated whether the SSRI paroxetine could prevent HF progression in the post-MI mouse due to its GRK2 inhibitory action. This represents a “proof-of-concept” study not only for the potential use of paroxetine in depressed HF patients based on its micromolar affinity for GRK2 inhibition as an “off-target” but also for the therapeutic effectiveness of inhibiting systemic GRK2 activity in HF using small-molecule pharmacotherapy. Treatment with paroxetine was done for 4 weeks and was not started until HF was evident (2 weeks after MI). Paroxetine-mediated inhibition of GRK2 in vivo in the mouse is feasible, and it not only enhanced LV function after MI but also decreased ventricular remodeling in an SSRI-independent manner. The ability to deliver a small-molecule inhibitor that would temper GRK2 activity ubiquitously presents an intriguing avenue for treatment of human HF, especially because work over the last two decades has shown GRK2 to be a pathological driver of cardiac dysfunction (3, 5, 24).

Previously, we found in vitro and in vivo doses of paroxetine that could inhibit GRK2 and increase βAR-mediated cardiomyocyte contractility in normal mice and cells, and these doses supported the selective micromolar affinity for this molecule on GRK2 (18). Accordingly, we chose a dose of 5 mg/kg per day that should result in appropriate serum concentrations of paroxetine in the mouse (20–22). Indeed, we found levels of paroxetine in our treated mice that were equivalent to levels seen in humans treated with this SSRI for depression. Of translational relevance, our findings strongly suggest that the reversal of HF and adverse LV remodeling in the post-MI mouse are directly a result of GRK2 inhibition and not the SSRI activity of paroxetine. First, equivalent doses of a second SSRI, fluoxetine, did nothing to the post-MI HF phenotype, and responses were identical to vehicle treatment. Second, the central effects of paroxetine and SSRIs in general are not evident for weeks (21), and we found measureable beneficial effects 2 weeks after treatment. Last, cardiac functional improvement and reversal of adverse LV remodeling seen with paroxetine were similar to our previous findings with inducible cardiac-specific GRK2 knockout mice, where GRK2 was not ablated in the mouse until after MI (23). Therefore, paroxetine appears to have a specific cardiac effect in the post-MI mouse, which we propose could lead to drug repurposing or a medicinal chemistry starting point to develop a new class of HF drugs targeting GRK2.

In treatment of human HF, it is important to see a persistent beneficial effect or biochemical alteration in the myocardium. We were encouraged to find that the therapeutic benefit of paroxetine treatment from 2 to 6 weeks after MI was not lost upon removing paroxetine therapy from weeks 6 to 8 after MI. These data suggest that paroxetine treatment can induce a lasting effect on the myocardium, independent of its continued presence. We suggest that this occurs because GRK2 inhibition through paroxetine will act not only on up-regulated GRK2 to provide feedback on catecholamine levels in the heart but also within the SNS

where abnormal GRK2 activity is known to promote catecholamine release and targeted inhibition of GRK2 in the adrenal gland can lower catecholamine release (3, 25). Indeed, chronic treatment with paroxetine, but not fluoxetine, decreased plasma catecholamine levels to sham levels, and the myocardial βAR system was normalized including decreased GRK2 levels. Moreover, plasma catecholamines stayed low 2 weeks after cessation of treatment, and thus, the βAR-mediated inotropic reserve stays intact.

In addition to the above, any new HF therapy must demonstrate a beneficial effect greater than the current standard-of-care therapy. It was therefore important to compare paroxetine treatment to β-blocker therapy and investigate whether coadministration could provide any additive therapeutic benefit. Consistent with other studies, the clinically used β_1-AR antagonist metoprolol alone did halt the progression of LV dysfunction after MI, but did not enhance function (13). In contrast, paroxetine alone or as a cotherapy with metoprolol not only blocks disease progression but also significantly improves LV function, preserves myocardial structure, and reverses HF. Moreover, paroxetine alone as well as paroxetine and metoprolol together were superior at decreasing molecular biomarkers of HF including BNP and GRK2. Regardless of mechanism, our study demonstrates that paroxetine can have profound and lasting effects in the post-MI heart that are SSRI-independent and are consistent with GRK2 inhibition. Previously, we have targeted GRK2 in the heart with the βARKct using transgenic mice (9) or viral-mediated gene therapy (12–14), or also with cardiac-specific GRK2 gene deletion (23), to prevent or reverse the HF phenotype. However, the use of a small-molecule inhibitor of GRK2 would have advantages over myocardial gene therapy primarily because, as discussed above, it would also target the known abnormal SNS activity of GRK2 (3). This could also be the mechanism behind its apparent superiority over β-blockade because inhibiting cardiac βARs may lead to an indirect sympatholytic effect over time, whereas inhibiting systemic GRK2 activity would provide direct sympatholytic effect, which appears to be the case (25). Notably, there have been recent reports of small-molecule inhibitors of the Gβγ-mediated membrane translocation of GRK2 (24) being effective in rescuing other models of HF in mice, including having direct sympatholytic activity (26); however, these compounds have issues regarding their suitability for proceeding down the drug development path and do not selectively target GRK2 activity (24). The Food and Drug Administration–approved status of paroxetine increases the potential attractiveness of developing this agent as a GRK2 inhibitor in patients with both HF and depression or using its chemical structure as a platform for further drug development (27).

GRK2 inhibition and its positive role in preserving cardiac structure and function after MI may also involve emerging mechanisms of GRK2-mediated pathology. These include GRK2 having a negative effect on insulin signaling and glucose metabolism in myocardium (25, 28) and on the regulation of nitric oxide synthase activity (29) and mitochondrial function (16), which contribute to the pro-death activity of GRK2 (15–17). Therefore, inhibition of GRK2 can not only improve cardiac contractility through adrenergic means but also preserve protective signaling pathways.

Paroxetine is approved and marketed for use in treating patients with a number of depression- and anxiety-related disorders (30, 31). A wealth of data is available from clinical

trials and postclinical application regarding human bioavailability, toxicity, adverse effects, and contraindications. There already are clinically and translationally important data concerning paroxetine and HF. HF patients are often depressed, and trials have shown that paroxetine along with other SSRIs can be used effectively to treat depression in these patients (32–34). Although this therapy certainly improves mental outlook and data have shown improvement in patient outcomes and quality of life (32–34), specific improvements in cardiac function have not been evaluated.

Overall, treatment of human subjects with paroxetine as a means to improve cardiovascular function after MI would represent a new indication for the drug. However, caution needs to be applied here because our data are only in the mouse, where higher doses are possible. It is probable that chronic paroxetine treatment in nondepressed HF patients, especially at doses needed to inhibit GRK2, would not be practical. However, studying the chemical entity and its binding sites within the catalytic domain of GRK2 represents an innovative starting point for medicinal chemistry development of a class of selective GRK2 inhibitors.

In summary, we demonstrate in a mouse model of post-MI HF that a dose of the SSRI antidepressant paroxetine, at serum levels comparable to those seen in patients treated for depression, can markedly improve LV function and structure, reverse the reexpression of the maladaptive fetal gene program that characterizes HF in both animal models and humans, lower adrenergic drive, and lower GRK2 levels. These beneficial effects were drug-specific and greater than that seen with the β-blocker metoprolol. In aggregate, our data strongly support the concept that GRK2 can serve as a target for the development of new therapies for the treatment of HF. Moreover, the present data, albeit in a mouse model, provide a strong rationale for evaluating the cardiac effects of paroxetine as compared to other SSRIs in a large number of patients with HF and the comorbidity of depression.

MATERIALS AND METHODS

Study design

Our central hypothesis was that selective inhibition of GRK2 by the SSRI paroxetine would improve cardiac function in HF, preserve βAR sensitivity, and prevent adverse remodeling after MI. After initiation of data analysis, our secondary hypothesis was that the significant biochemical improvements achieved by paroxetine treatment would result in a persistent beneficial effect upon termination of treatment. Statistical powering was initially performed using the nQuery Advisor 3.0 software (Statistical Solutions) for estimation of sample size. For all experiments, the calculations use $\alpha = 0.05$ and $\beta = 0.2$ (power = 0.80). On the basis of these calculations, our target was a minimum of 5 animals (powered for indices of myocardial function) per MI group to attain statistical significance, with a preference for 10 or more. Each experiment was performed a minimum of three times, with some performed up to seven times. The number and composition of the replicates were determined on the basis of availability of the surgeon, echocardiography, and hemodynamic equipment, as well as the survival rate after MI and equal randomized enrollment to the treatment groups upon confirmation of MI by echocardiography 2 weeks after surgery. The 6-week endpoint and serial measures were parts of the initial study design, with the 8-week endpoint added on the basis of our findings. All animals and resulting samples were monitored by mouse number

only until data quantification was complete. Data were then decoded to the assigned treatment groups for statistical analysis. Serum catecholamine and βAR receptor density analyses were performed by external groups who only received mouse number identification. All results were substantiated by repetition. Data were only excluded if their validity was undermined by the condition of the animal or cells before or during the experiment, such as loss of the specimen.

Experimental animals and materials

The wild-type C57BL/6 male mice used for this study were obtained from The Jackson Laboratory. All animal procedures were carried out according to the National Institutes of Health (NIH) *Guide for the Care and Use of Laboratory Animals* and approved by the Animal Care and Use Committee of Temple University.

In vivo ischemic injury protocols

For our MI model, mice were subjected to permanent ligation of the left main descending coronary artery or a sham surgery as we have described (19). There is a 20 to 30% mortality rate within the first week after this procedure (before any treatment), after which all mice survived to the 6- or 8-week endpoints of this study. Trichrome staining was performed as previously described (19). Western blotting was performed as described previously (29).

Mini osmotic pumps

Chronic infusion of vehicle (DMSO in water or water), paroxetine or fluoxetine (5 mg/kg per day), metoprolol (250 mg/kg per day), or metoprolol and paroxetine (250 and 5 mg/kg per day, respectively) was achieved using ALZET 2-week osmotic minipumps (model 1002, DURECT Corp.) implanted subcutaneously.

Serum paroxetine and catecholamines

Quantification of paroxetine from mouse serum was performed by liquid chromatography–tandem mass spectrometry (LC-MS/MS) using an AB SCIEX API 5000 connected to a Shimadzu HPLC (high-performance liquid chromatography) 20AD with a C18 column (50 mm × 3 mm, 3 μm). The calibration range was 1 to 500 ng/ml using 0.25 ml of serum. Quantification of epinephrine and norepinephrine from mouse serum was performed through LC-MS/MS using an AB SCIEX API 6500 connected to a Shimadzu HPLC 30AD with a C18 HPLC column (50 mm × 2.1 mm, 3 μm). The calibration range was 10 to 2000 pg/ml using 0.25 ml of serum.

Membrane preparation and radioligand binding assay for βARs

After membrane preparation, radioligand [^{125}I]CYP (PerkinElmer, iodo-(−)-cyanopindolol, [^{125}I], NEX189100UC and NEX310010UC) binding to βARs was measured, and K_d (dissociation constant) and the maximal number of binding sites (B_{max}) for [^{125}I]CYP were determined by Scatchard analysis of saturation binding isotherms with GraphPad Prism as described (35).

RNA isolation and semiquantitative PCR

RNA isolation and analysis were performed as previously described (29). Semiquantitative PCR was carried out on complementary DNA using SYBR Green (Bio-Rad) and 100 nM gene-specific oligonucleotides for 18*S* and ANF on a CFX96 real-time system with Bio-Rad CFX Manager 2.1 software. Quantitation was established by comparing 18*S* ribosomal RNA, which was similar between groups, for normalization and compared using the $\Delta\Delta C_t$ method.

Statistical analysis

All values in the text and figures are presented as means ± SEM of independent experiments for given *n* sizes. Statistical significance was determined by one-way ANOVA with Tukey or two-way ANOVA with Bonferroni post hoc as appropriate. Probabilities of 0.05 or less were considered to be statistically significant.

Supplementary Material

Refer to Web version on PubMed Central for supplementary material.

Acknowledgments

We thank Z. Qu and S. Baxter for technical assistance.

Funding: This work was supported by a Brody Family Medical Trust Fund Fellowship (S.M.S.) and NIH grants HL086865 (J.J.G.T.), R37 HL061690 (W.J.K.), P01 HL08806 (W.J.K.), P01 HL075443 (W.J.K.), and P01 HL091799 (W.J.K, W.Z., and A.M.F).

REFERENCES AND NOTES

1. Dunlay SM, Pereira NL, Kushwaha SS. Contemporary strategies in the diagnosis and management of heart failure. Mayo Clin Proc. 2014; 89:662–676. [PubMed: 24684781]
2. Bristow MR, Ginsburg R, Minobe W, Cubicciotti RS, Sageman WS, Lurie K, Billingham ME, Harrison DC, Stinson EB. Decreased catecholamine sensitivity and β-adrenergic-receptor density in failing human hearts. N Engl J Med. 1982; 307:205–211. [PubMed: 6283349]
3. Lymperopoulos A, Rengo G, Koch WJ. Adrenergic nervous system in heart failure: Pathophysiology and therapy. Circ Res. 2013; 113:739–753. [PubMed: 23989716]
4. Claing A, Laporte SA, Caron MG, Lefkowitz RJ. Endocytosis of G protein-coupled receptors: Roles of G protein-coupled receptor kinases and β-arrestin proteins. Prog Neurobiol. 2002; 66:61–79. [PubMed: 11900882]
5. Rockman HA, Koch WJ, Lefkowitz RJ. Seven-transmembrane-spanning receptors and heart function. Nature. 2002; 415:206–212. [PubMed: 11805844]
6. Ungerer M, Böhm M, Elce JS, Erdmann E, Lohse MJ. Altered expression of beta-adrenergic receptor kinase and beta 1-adrenergic receptors in the failing human heart. Circulation. 1993; 87:454–463. [PubMed: 8381058]
7. Iaccarino G, Barbato E, Cipolletta E, De Amicis V, Margulies KB, Leosco D, Trimarco B, Koch WJ. Elevated myocardial and lymphocyte GRK2 expression and activity in human heart failure. Eur Heart J. 2005; 26:1752–1758. [PubMed: 16055494]
8. Koch WJ, Rockman HA, Samama P, Hamilton RA, Bond RA, Milano CA, Lefkowitz RJ. Cardiac function in mice overexpressing the beta-adrenergic receptor kinase or a beta ARK inhibitor. Science. 1995; 268:1350–1353. [PubMed: 7761854]

9. Rockman HA, Chien KR, Choi DJ, Iaccarino G, Hunter JJ, Ross J Jr, Lefkowitz RJ, Koch WJ. Expression of a β-adrenergic receptor kinase 1 inhibitor prevents the development of myocardial failure in gene-targeted mice. Proc Natl Acad Sci USA. 1998; 95:7000–7005. [PubMed: 9618528]
10. Akhter SA, Eckhart AD, Rockman HA, Shotwell K, Lefkowitz RJ, Koch WJ. In vivo inhibition of elevated myocardial β-adrenergic receptor kinase activity in hybrid transgenic mice restores normal β-adrenergic signaling and function. Circulation. 1999; 100:648–653. [PubMed: 10441103]
11. Harding VB, Jones LR, Lefkowitz RJ, Koch WJ, Rockman HA. Cardiac βARK1 inhibition prolongs survival and augments β blocker therapy in a mouse model of severe heart failure. Proc Natl Acad Sci USA. 2001; 98:5809–5814. [PubMed: 11331748]
12. Shah AS, White DC, Emani S, Kypson AP, Lilly RE, Wilson K, Glower DD, Lefkowitz RJ, Koch WJ. In vivo ventricular gene delivery of a β-adrenergic receptor kinase inhibitor to the failing heart reverses cardiac dysfunction. Circulation. 2001; 103:1311–1316. [PubMed: 11238278]
13. Rengo G, Lymperopoulos A, Zincarelli C, Donniacuo M, Soltys S, Rabinowitz JE, Koch WJ. Myocardial adeno-associated virus serotype 6–βARKct gene therapy improves cardiac function and normalizes the neurohormonal axis in chronic heart failure. Circulation. 2009; 119:89–98. [PubMed: 19103992]
14. Raake PW, Schlegel P, Ksienzyk J, Reinkober J, Barthelmes J, Schinkel S, Pleger S, Mier W, Haberkorn U, Koch WJ, Katus HA, Most P, Müller OJ. AAV6.βARKct cardiac gene therapy ameliorates cardiac function and normalizes the catecholaminergic axis in a clinically relevant large animal heart failure model. Eur Heart J. 2013; 34:1437–1447. [PubMed: 22261894]
15. Brinks H, Boucher M, Gao E, Chuprun JK, Pesant S, Raake PW, Huang ZM, Wang X, Qiu G, Gumpert A, Harris DM, Eckhart AD, Most P, Koch WJ. Level of G protein–coupled receptor kinase-2 determines myocardial ischemia/reperfusion injury via pro- and anti-apoptotic mechanisms. Circ Res. 2010; 107:1140–1149. [PubMed: 20814022]
16. Chen M, Sato PY, Chuprun JK, Peroutka RJ, Otis NJ, Ibetti J, Pan S, Sheu SS, Gao E, Koch WJ. Prodeath signaling of G protein–coupled receptor kinase 2 in cardiac myocytes after ischemic stress occurs via extracellular signal–regulated kinase-dependent heat shock protein 90–mediated mitochondrial targeting. Circ Res. 2013; 112:1121–1134. [PubMed: 23467820]
17. Fan Q, Chen M, Zuo L, Shang X, Huang MZ, Ciccarelli M, Raake P, Brinks H, Chuprun KJ, Dorn GW II, Koch WJ, Gao E. Myocardial ablation of G protein–coupled receptor kinase 2 (GRK2) decreases ischemia/reperfusion injury through an anti-intrinsic apoptotic pathway. PLOS One. 2013; 8:e66234. [PubMed: 23805205]
18. Thal DM, Homan KT, Chen J, Wu EK, Hinkle PM, Huang ZM, Chuprun JK, Song J, Gao E, Cheung JY, Sklar LA, Koch WJ, Tesmer JJ. Paroxetine is a direct inhibitor of G protein-coupled receptor kinase 2 and increases myocardial contractility. ACS Chem Biol. 2012; 7:1830–1839. [PubMed: 22882301]
19. Gao E, Lei YH, Shang X, Huang ZM, Zuo L, Boucher M, Fan Q, Chuprun JK, Ma XL, Koch WJ. A novel and efficient model of coronary artery ligation and myocardial infarction in the mouse. Circ Res. 2010; 107:1445–1453. [PubMed: 20966393]
20. Kirchherr H, Kühn-Velten WN. Quantitative determination of forty-eight antidepressants and antipsychotics in human serum by HPLC tandem mass spectrometry: A multi-level, single-sample approach. J Chromatogr B Analyt Technol Biomed Life Sci. 2006; 843:100–113.
21. Meyer JH, Wilson AA, Ginovart N, Goulding V, Hussey D, Hood K, Houle S. Occupancy of serotonin transporters by paroxetine and citalopram during treatment of depression: A [^{11}C]DASB PET imaging study. Am J Psychiatry. 2001; 158:1843–1849. [PubMed: 11691690]
22. Tasker TC, Kaye CM, Zussman BD, Link CG. Paroxetine plasma levels: Lack of correlation with efficacy or adverse events. Acta Psychiatr Scand Suppl. 1989; 350:152–155. [PubMed: 2530776]
23. Raake PW, Vinge LE, Gao E, Boucher M, Rengo G, Chen X, DeGeorge BR Jr, Matkovich S, Houser SR, Most P, Eckhart AD, Dorn GW II, Koch WJ. G protein–coupled receptor kinase 2 ablation in cardiac myocytes before or after myocardial infarction prevents heart failure. Circ Res. 2008; 103:413–422. [PubMed: 18635825]
24. Casey LM, Pistner AR, Belmonte SL, Migdalovich D, Stolpnik O, Nwakanma FE, Vorobiof G, Dunaevsky O, Matavel A, Lopes CM, Smrcka AV, Blaxall BC. Small molecule disruption of Gβγ

signaling inhibits the progression of heart failure. Circ Res. 2010; 107:532–539. [PubMed: 20576935]

25. Lymperopoulos A, Rengo G, Funakoshi H, Eckhart AD, Koch WJ. Adrenal GRK2 upregulation mediates sympathetic overdrive in heart failure. Nat Med. 2007; 13:315–323. [PubMed: 17322894]
26. Kamal FA, Mickelsen DM, Wegman KM, Travers JG, Moalem J, Hammes SR, Smrcka AV, Blaxall BC. Simultaneous adrenal and cardiac G-protein–coupled receptor-Gβγ inhibition halts heart failure progression. J Am Coll Cardiol. 2014; 63:2549–2557. [PubMed: 24703913]
27. Homan KT, Wu E, Wilson MW, Singh P, Larsen SD, Tesmer JJ. Structural and functional analysis of G protein–coupled receptor kinase inhibition by paroxetine and a rationally designed analog. Mol Pharmacol. 2014; 85:237–248. [PubMed: 24220010]
28. Ciccarelli M, Chuprun JK, Rengo G, Gao E, Wei Z, Peroutka RJ, Gold JI, Gumpert A, Chen M, Otis NJ, Dorn GW II, Trimarco B, Iaccarino G, Koch WJ. G protein–coupled receptor kinase 2 activity impairs cardiac glucose uptake and promotes insulin resistance after myocardial ischemia. Circulation. 2011; 123:1953–1962. [PubMed: 21518983]
29. Huang ZM, Gao E, Fonseca FV, Hayashi H, Shang X, Hoffman NE, Chuprun JK, Tian X, Tilley DG, Madesh M, Lefer DJ, Stamler JS, Koch WJ. Convergence of G protein–coupled receptor and S-nitrosylation signaling determines the outcome to cardiac ischemic injury. Sci Signal. 2013; 6:ra95. [PubMed: 24170934]
30. Mandrioli R, Mercolini L, Saracino MA, Raggi MA. Selective serotonin reuptake inhibitors (SSRIs): Therapeutic drug monitoring and pharmacological interactions. Curr Med Chem. 2012; 19:1846–1863. [PubMed: 22414078]
31. Gibiino S, Serretti A. Paroxetine for the treatment of depression: A critical update. Expert Opin Pharmacother. 2012; 13:421–431. [PubMed: 22263916]
32. Gottlieb SS, Kop WJ, Thomas SA, Katzen S, Vesely MR, Greenberg N, Marshall J, Cines M, Minshall S. A double-blind placebo-controlled pilot study of controlled-release paroxetine on depression and quality of life in chronic heart failure. Am Heart J. 2007; 153:868–873. [PubMed: 17452166]
33. Chittaranjan A, Chethan KB, Sandarsh S. Cardiovascular mechanisms of SSRI drugs and their benefits and risks in ischemic heart disease and heart failure. Int Clin Psychopharmacol. 2013; 28:145–155. [PubMed: 23325305]
34. Silver MA. Depression and heart failure: An overview of what we know and don't know. Cleve Clin J Med. 2010; 77(Suppl 3):S7–S11. [PubMed: 20622081]
35. Kitagawa Y, Adachi-Akahane S, Nagao T. Determination of beta-adrenoceptor subtype on rat isolated ventricular myocytes by use of highly selective beta-antagonists. Br J Pharmacol. 1995; 116:1635–1643. [PubMed: 8564230]

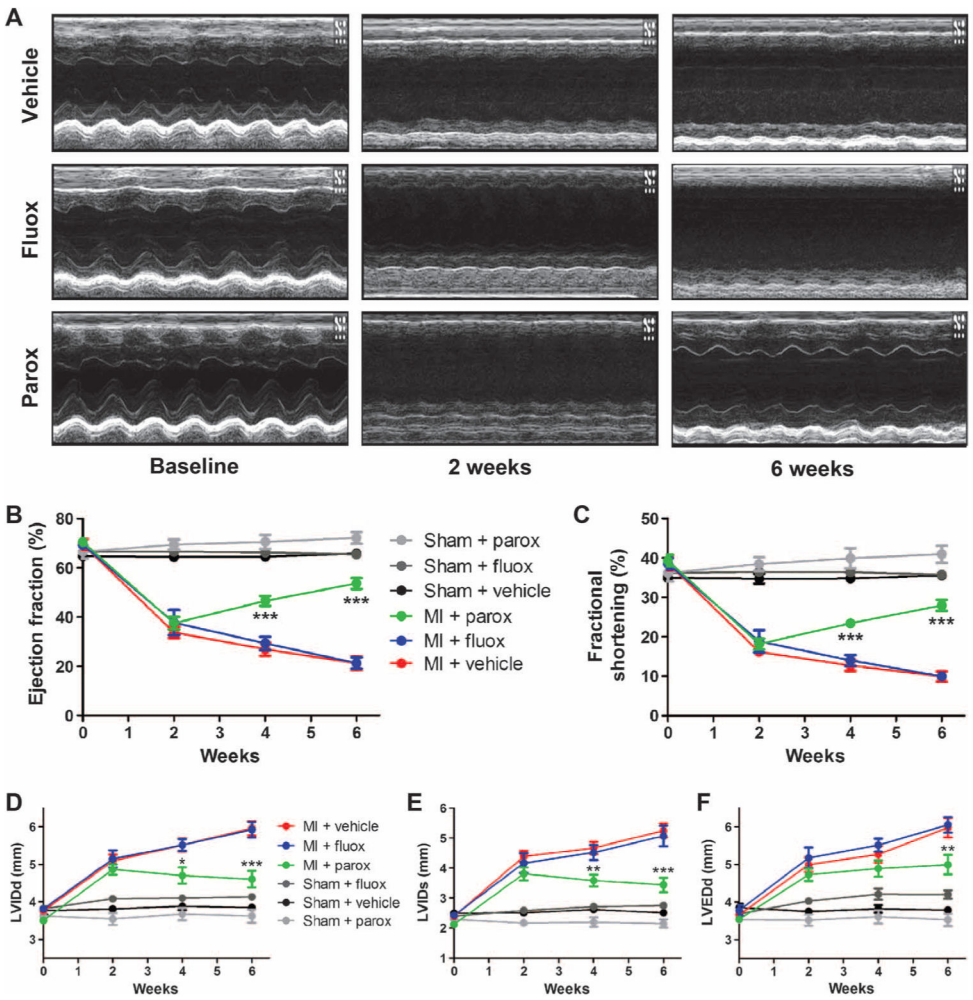

Fig. 1. Paroxetine treatment reverses LV dysfunction after MI

(**A**) Representative short-axis M-mode echocardiography recordings from C57BL/6 mice treated with vehicle (DMSO and water), fluoxetine (fluox), or paroxetine (parox) at baseline, 2 weeks (pretreatment) and 4 and 6 weeks after MI compared to noninfarcted (sham) mice treated the same way. (**B** and **C**) Serial measures of noted experimental groups for (B) LVEF and (C) FS. (**D** and **E**) Serial measures of (D) LVIDd and (E) LVIDs in these mice. (**F**) Serial measures of LVEDd in these mice. **P* = 0.004, ***P* = 0.001, ****P* < 0.0001 as determined by one-way analysis of variance (ANOVA) relative to corresponding MI vehicle. *n* = 9 to 14 per group.

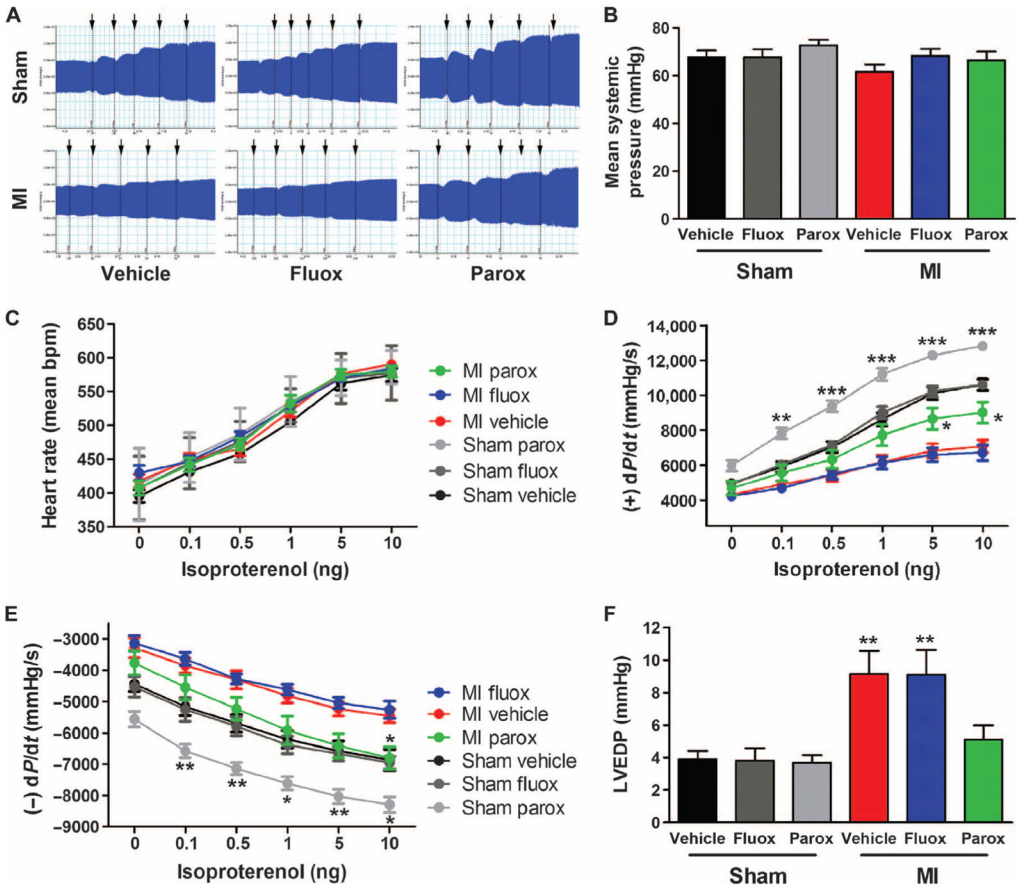

Fig. 2. Paroxetine treatment after MI enhances in vivo LV hemodynamic function and restores βAR inotropic reserve

.
Hemodynamics were recorded from wild-type (WT) mice treated with vehicle, fluoxetine (fluox), or paroxetine (parox) at 6 weeks after MI (after 4 weeks of treatment) compared to sham. (**A**) Representative LV d*P*/d*t* hemodynamic recordings. Arrows mark administration of ISO. (**B**) Quantification of mean systemic pressure. (**C** to **E**) Quantification of (C) HR, (D) LV +d*P*/d*t* average maximum (**P* = 0.0234 and 0.0130, ***P* = 0.0008, ****P* ≤ 0.0001), and (E) LV −d*P*/d*t* average minimum at baseline and with increasing doses of ISO (0.1 to 10 ng) (**P* = 0.0105 and 0.0134 for sham, and 0.0280 for MI; ***P* = 0.0058, 0.0040, and 0.0087, respectively). bpm, beats per minute. (**F**) Quantification of LVEDP at baseline (no ISO) 6 weeks after sham and MI (***P* = 0.005). Statistics are relative to corresponding sham or MI vehicle by two-or one-way ANOVA as appropriate. *n* = 12 to 15 per group.

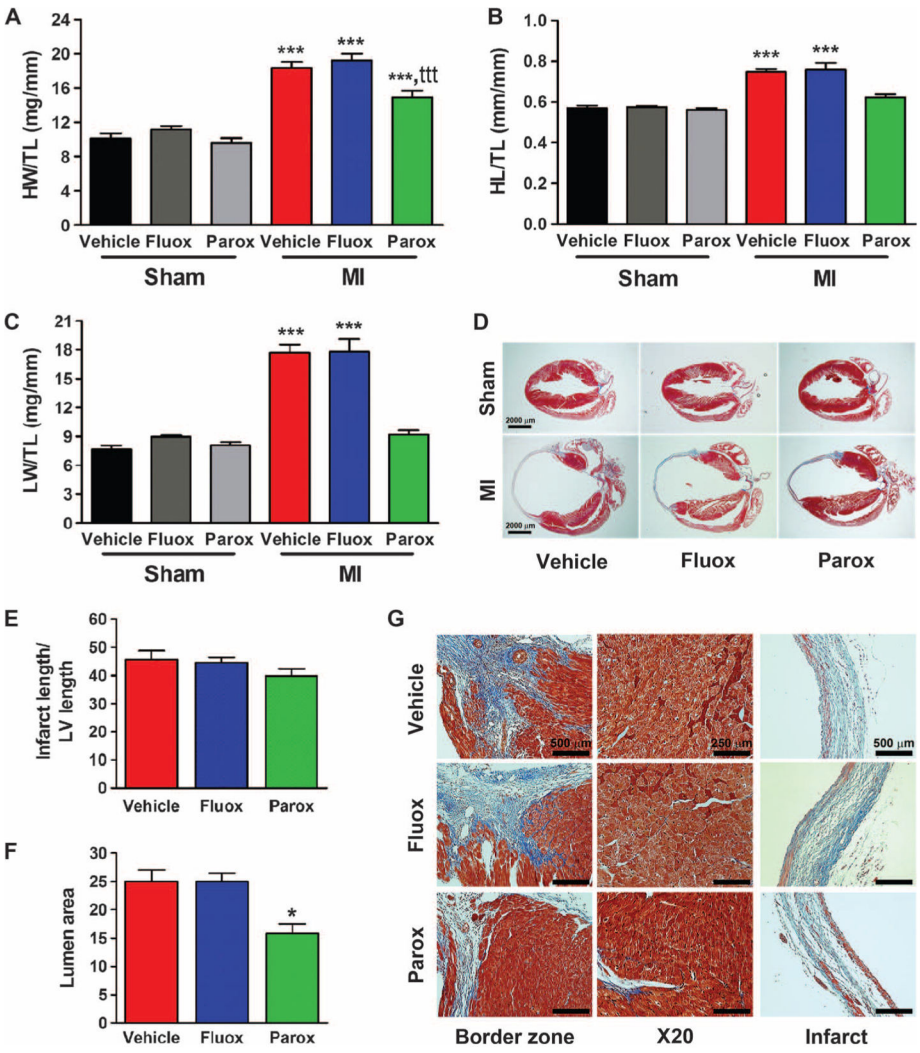

Fig. 3. Paroxetine reduces LV dilation and fibrosis after MI

(**A** to **C**) Measures of (A) HW normalized to TL, (B) HL normalized to TL, and (C) LW to TL in WT C57BL/6 mice treated with vehicle, fluoxetine (fluox), or paroxetine (parox) at 6 weeks after MI (4 weeks of treatment) compared to noninfarcted (sham) mice treated the same way. ***$P \leq 0.0001$ relative to sham and $^{ttt}P = 0.0075$ relative to MI vehicle by one-way ANOVA. $n = 12$ to 19 per group. (**D**) Representative images of Masson's trichrome–stained murine heart sections from WT mice treated with vehicle, fluox, or parox at 6 weeks after sham or MI surgery (4 weeks after treatment). (**E** and **F**) Graphic representation of (E) infarct length and (F) lumen area in vehicle-, fluox-, or parox-treated mice 6 weeks after MI. *$P = 0.004$ by one-way ANOVA. $n = 7$, 6, and 8, respectively, for (D) to (G). (**G**) Representative images of Masson's trichrome–stained murine heart sections focusing on the border zone and the infarct area in vehicle-, fluox-, and parox-treated mice 6 weeks after MI.

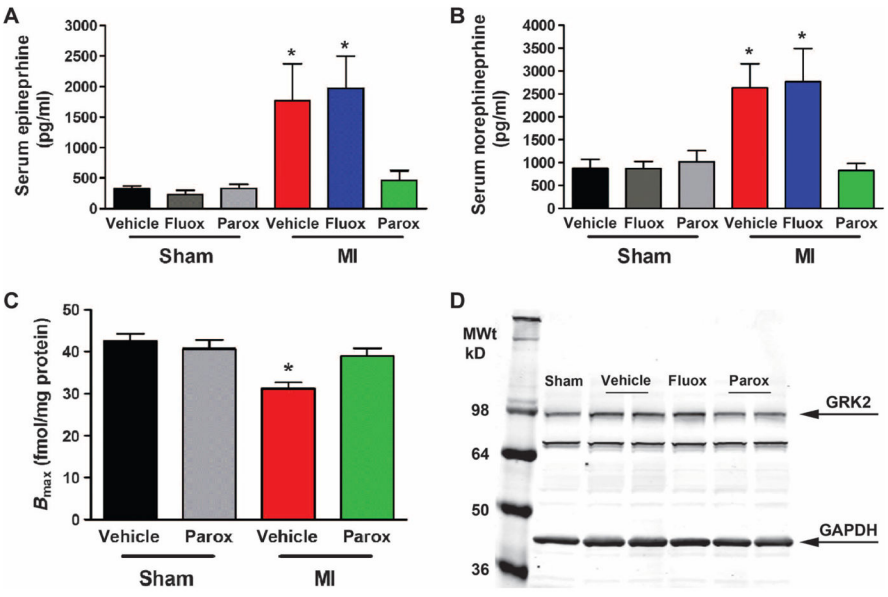

Fig. 4. Paroxetine reduces SNS overdrive and restores the myocardial βAR system after MI

(**A** and **B**) Quantification of serum (A) epinephrine and (B) norepinephrine from WT mice, either sham or MI at 6 weeks, treated with vehicle, fluoxetine (fluox), or paroxetine (parox). (**C**) βAR density in sham versus 6-week post-MI hearts (B_{max} values shown as femtomoles of receptor per milligram of sarcolemmal protein) with vehicle or parox treatment. (**D**) Representative Western blot image of GRK2 and GAPDH (glyceraldehyde-3-phosphate dehydrogenase) protein expression 6 weeks after sham or MI (after 4 weeks of treatment with vehicle, fluox, or parox). **P* = 0.0167, 0.0047, 0.0427, and 0.0244, respectively (A and B), and **P* = 0.0003 (C) versus sham vehicle and **P* = 0.0119 versus MI parox by one-way ANOVA. *n* = 6 to 9 per group.

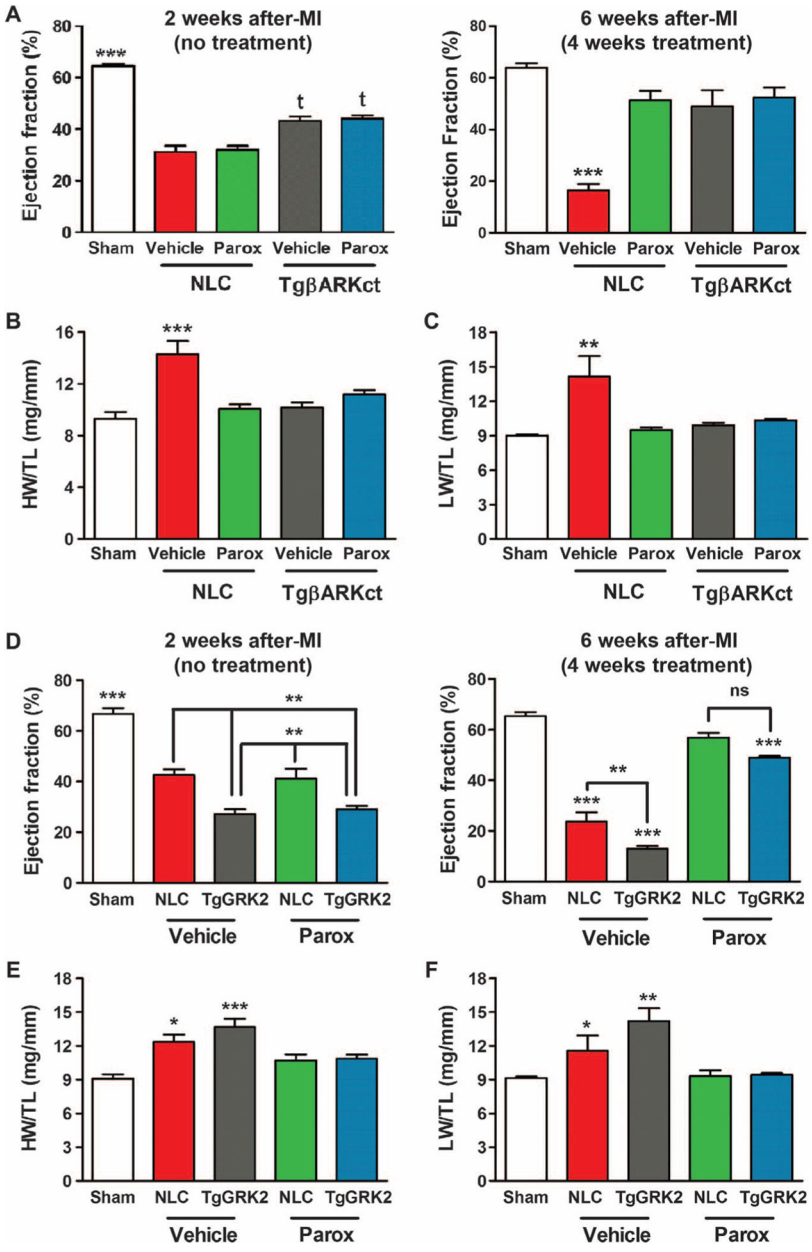

Fig. 5. Paroxetine's efficacy in reversing HF is not additive when GRK2 is inhibited by βARKct but is maintained even in the face of forced GRK2 overexpression

(**A**) Measures of LVEF at 2 (left) and 6 (right) weeks after MI in TgβARKct or NLC mice treated with vehicle or paroxetine (parox) compared to sham animals. ***$P < 0.0001$ relative to sham; $^{t}P = 0.0004$ or $P < 0.0001$ relative to NLC MI vehicle by one-way ANOVA of all 2-week or all 6-week data. (**B** and **C**) Measures of (B) HW and (C) LW normalized to TL in TgβARKct or NLC mice 6 weeks after MI compared to sham controls. **$P = 0.0027$; ***$P = 0.0001$ by one-way ANOVA. $n = 4$ to 8 per group. (**D**) Measures of LVEF at 2 (left) and 6 (right) weeks after MI in TgGRK2 or NLC mice treated with vehicle or parox compared to sham animals. **$P = 0.0001$, 0.0019, 0.0016, 0.0138, and 0.0019, respectively, relative to NLC MI vehicle or parox; ***$P < 0.0001$ relative to sham by one-

way ANOVA of all 2-week or all 6-week data. ns, not significant. (**E** and **F**) Measures of (E) HW/TL and (F) LW/TL in TgGRK2 or NLC mice 6 weeks after MI compared to sham controls. **P* = 0.0121 (E), 0.0412 (F); ***P* = 0.0025; ****P* < 0.0001 by one-way ANOVA. *n* = 5 to 11 per group.

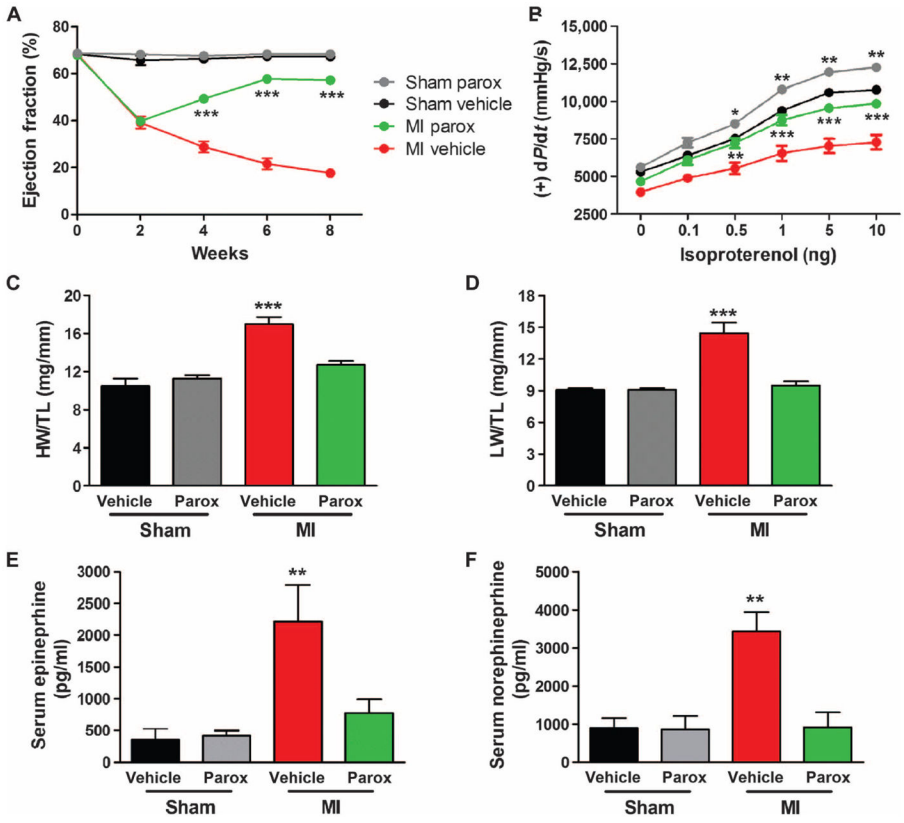

Fig. 6. Paroxetine's beneficial effect in post-MIHF is maintained after termination of treatment

C57BL/6 mice treated with vehicle (DMSO and water) or paroxetine (parox) at baseline, 2, 4, 6, and 8 weeks after procedure (sham and MI). Two weeks after surgery, these mice were treated with vehicle or paroxetine (parox) for 4 weeks (weeks 2 to 6), followed by an additional 2 weeks of no treatment (weeks 6 to 8). **(A)** Serial measures of noted experimental groups for LVEF. **(B)** Quantification of LV +d*P*/d*t* average maximum at baseline and with increasing doses of ISO (0.1 to 10 ng) in these mice. (**C**and **D**) Measures of (C) HW/TL and (D) LW/TL in these mice. (**E** and **F**) Quantification of serum (E) epinephrine and (F) norepinephrine in these mice. **P* = 0.0461; ***P* ≤ 0.0009 for (B) sham and (E); ***P* = 0.0072 for (B) MI and 0.0024 for (F); and ****P* ≤ 0.001 versus corresponding sham or MI by one- or two-way ANOVA as appropriate. *n* = 9 to 15 per group [(A) to (D)], *n* = 4 to 5 per group for serum catecholamines.

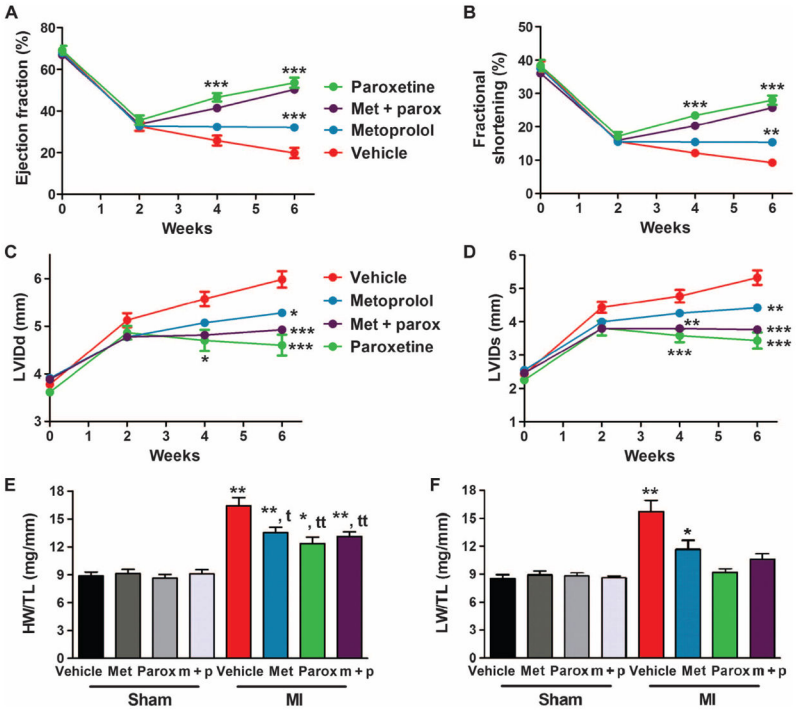

Fig. 7. Paroxetine is more effective at reversing post-MI HF than β-blocker therapy alone

(**A** and **B**) Serial measures of LVEF (**A**) and FS (B) from WT mice treated with vehicle, metoprolol (met), paroxetine (parox), or metoprolol and paroxetine concurrently after MI compared to vehicle-treated mice. ***P* = 0.0011 and ****P* < 0.001 by one-way ANOVA for post-MI parox and met + parox or met relative to corresponding MI vehicle and met. (**C** and **D**) Serial measures of (C) LVIDd and (D) LVIDs in these animals compared to sham mice. **P* = 0.0012 parox and 0.0047 m + p (4 weeks), 0.0116 (6 weeks met); ***P* = 0.0005 m + p and 0.0015 met; ****P* < 0.0001 by one-way ANOVA relative to MI vehicle. (**E** and **F**) Measures of (E) HW and (F) LW normalized to TL 6 weeks after MI or sham. **P* = 0.0001 (HW), 0.0246 (LW); ***P* < 0.0001 relative to sham and ^{t}P = 0.0349; ^{tt}P = 0.0045 parox and 0.0077 m + p relative to MI vehicle by one-way ANOVA. *n* = 4 (met, m + p sham), 13 to 18 all other groups.

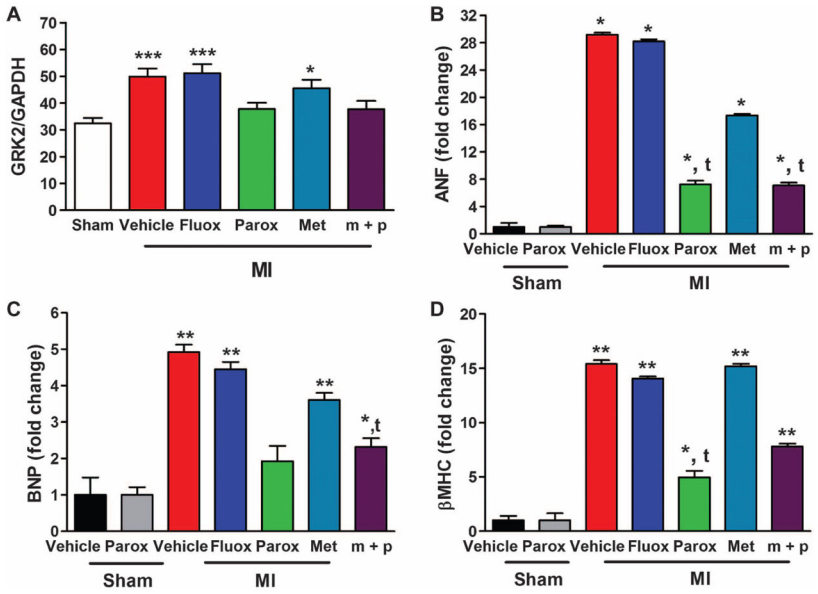

Fig. 8. Paroxetine decreases molecular markers of HF in post-MI mice

Analysis of WT murine hearts treated with vehicle, fluoxetine (fluox), paroxetine (parox), metoprolol (met), or metoprolol and paroxetine (m + p) at 6 weeks after MI compared to sham mice treated with vehicle or parox. (**A**) Quantification of GRK2 protein expression normalized to GAPDH from Western blots. **P* = 0.0073; ****P* = 0.0002 and 0.0004 by one-way ANOVA compared to sham values. *n* = 9 to 17 hearts per group from seven Western blots. (**C** to **D**) Quantification of RT-PCR data showing fold change in (B) ANF **P* < 0.0001 except parox = 0.0008 and ^{t}P = 0.0145 parox and 0.0006 m + p; (C) BNP **P* = 0.0458, ***P* < 0.0001 except met 0.0004, ^{t}P = 0.0223; and (D) βMHC mRNA expression in **P* = 0.0052, ***P* < 0.0001; ^{t}P = 0.0383. All * relative to sham vehicle and t versus post-MI vehicle by one-way ANOVA. *n* = 6 to 14 per group.